

Radiant heat exchange mediated by gaseous atmosphere

C. A. Duarte

Received: 28 December 2010 / Accepted: 2 August 2011 / Published online: 21 August 2011
© Akadémiai Kiadó, Budapest, Hungary 2011

Abstract As is well known, the heat exchange between bodies at different temperatures enclosed at vacuum without thermal contact can be described by the Stefan–Boltzmann law of radiation, where each body receives a fraction of radiant heat from the others depending on their distances and individual temperatures, geometrical shapes, emissivities, and absorptivities. However, when these bodies are surrounded by a gaseous atmosphere conductive and convective phenomena enter on the scenario, leading to a complex mechanism of heat exchange. Here, we study an experimental realization of such situation for two bodies employing a kind of vacuum gauge, on a range of surrounding air pressure between 26 and 1035 mbar, and analyze the heat exchange on the framework of Stefan–Boltzmann law. It is verified empirically that the ratio between the thermal power irradiated by the bodies is independent on their individual heat radiances, and depends only on the surrounding gas pressure.

Keywords Stefan–Boltzmann law · Black body · Radiation · Convection · Vacuum

Introduction

Many pressure gauges operate with reference to the thermal properties of the residual gas in the vacuum system. As an example, the well-known Pirani [1–3] gauges measure with accuracy using the variation of electrical resistance of a filament immersed in the vacuum whose residual pressure

is being measured. Voege’s pressure gauge consisted of an electrically heated filament to the middle of which a thermocouple was soldered [4], and Steckelmacher presented a possible alternative, using natural and forced convection [5]. Recently, Duarte has shown a variant of Voege vacuum gauge, where the thermocouple is separated from the filament, allowing the measurement at ranges of pressure near the atmospheric pressure [6].

The operation of these vacuum gauges depends on the loss of heat of a hot filament to the surrounding gas, which in turn depends obviously on both the gas heat conductivity and the convective effects. We stress that this loss and exchanges of heat has a third important term associated to the thermal radiation, following the Stefan–Boltzmann law [7]. As is well known, the heat exchange between bodies at different temperatures enclosed at vacuum without thermal contact can be described by the Stefan–Boltzmann law of radiation, knowing their temperatures, cross sectional areas, emissivities, and total absorptivities. The underlying physics of thermal transfer becomes a complex phenomenon involving all these heat transfer processes, where while the irradiative contribution is governed simply by the Stefan–Boltzmann law. This phenomenon of radiant heat exchange recently received attention of some researchers [8]. In the situation, when there is a gaseous atmosphere as in this study the heat flux around the gas must be determined solving the Navier–Stokes equation with appropriate boundary conditions [9]. The Stefan–Boltzmann law together with the thermodynamics of heat machines was employed in the Ref. [10] which studied power systems propelled by heat and mass transfer. We stress that the transport of heat involving convection and conduction left to the creation of the new concept of entransy [11].

In this study, we study the influence of surrounding gas in the heat exchange between bodies, particularly

C. A. Duarte (✉)
Departamento de Física, Universidade Federal do Paraná,
CP 19044, Curitiba, PR 81531-990, Brazil
e-mail: celso@fisica.ufpr.br

analyzing the heat flow in a kind of vacuum gauge as above mentioned [6]. This study is organized as follows: we start presenting the underlying theoretical background on section Theory, where we state the Stefan–Boltzmann law and then dedicate our attention to the irradiative heat transfer between bodies to give theoretical background to our experimental investigations, presented in subsequent sections “Experimental” and “Results”. Then, we finish presenting final conclusions.

Theory

The Stefan–Boltzmann law governs the radiant emissivity of hot bodies, relating the radiant power emitted per surface area of a hot body (the energy emitted by the body by unit of time per unit of surface area) J to its temperature T by a fourth power law [7],

$$J = \sigma T^4, \quad (1)$$

where $\sigma = 5.67 \times 10^{-8} \text{ J s}^{-1} \text{ m}^{-2} \text{ K}^{-4}$ is the Stefan’s constant.

By the other side, if a very small object is irradiated by an energy flux W (energy by unit of time) emitted by a very small and distant heat source, it will absorb an amount of energy E by unit of time given by

$$E = F \cdot W, \quad (2)$$

where F is a dimensional number called *form factor*.

As a consequence, if such a very small object is initially cold, we can conclude from the laws of radiant heat that this object will be gradually heated by the small source and its temperature will converge gradually to a value T_o such that the rate of heat received from the source be equal to the heat that this object irradiates, which means a thermal equilibrium, or better, a stationary regime. We can determine the temperature of the irradiated object at this stationary regime using Eqs. 1 and 2. The radiant energy of the source E per unit time that reaches the object is

$$E = S_{\times} \cdot \frac{S_s}{4\pi d^2} J = \frac{S_{\times}}{4\pi d^2} W, \quad (3)$$

where S_s is the surface of the source, d is the distance between source and object, and S_{\times} is the cross-sectional area of the object perpendicular to the radius vector from source to object. From the above expression, we obtain $E = W \cdot S_{\times} / 4\pi d^2$, and as a consequence we can determine explicitly the form factor,

$$F = \frac{S_{\times}}{4\pi d^2}. \quad (4)$$

Then, if S_o is the total surface area of the object, E/S_o is just the radiant power emitted per surface area of the object

at the stationary regime, and by the Stefan–Boltzmann law is just σT_o^4 . As a consequence, aided by Eqs. 3 and 4 we reach to

$$S_o \cdot \sigma T_o^4 = F \cdot W. \quad (5)$$

If there are other sources, say $1, 2, \dots, N$ we have

$$E = \sum_{i=1}^N F_i \cdot W_i \quad (6)$$

and then,

$$\sigma T_o^4 = \sum_{i=1}^N f_i \cdot W_i, \quad (7)$$

where we have redefined the form factor of the object with respect to the i th source as $f_i = F_i/S_{o,i}$, being $S_{o,i}$ the cross-sectional area of the object perpendicular to the i th radius vector from the i th source to the object. Equation 6 naturally can be considered for the case when object and sources are not small, and the considered distances are not large. For that we simply must redefine the value of the individual form factors f_i with appropriate values to the particular geometry, and Eq. 7 continues to be valid.

Now, we may consider that the object and the sources are immersed in gaseous atmosphere at a fixed pressure. In this case, a fraction of the heat of the sources is transmitted to the gas by conduction, and the thermal expansion of the gas can develop a convective movement on the gas leaving out heat from the sources (and hot irradiated object). Each gas element of volume receiving heat from a source or from a neighbor hot gas element of volume expands and rises up, giving place to a cold gas element of volume which in turn passes by the same process. At stationary regime, the rate of heat left by the gas is a constant, even when sources, object and gas are enclosed in a closed cavity. In this later case, the heated gas warms the inner walls of the cavity, which has its temperature increased in turn causes an overall heating of all the system—sources, irradiated object, gas—until the stationary is achieved, when we verify a gradient of temperature along all the volume of the system. Of course, we have not such stationary regime if the sources cannot supply a constant rate of heat by undetermined period of time, but in this study we will treat the case when the source is a heat bath that can be considered as an infinite reservoir.

Of course we can imagine that the mathematical relation between all the heat rates—emitted and received—related to all the objects and the cavity obeys a linear relation as shown by Eq. 6. Nevertheless, the presence of a gas atmosphere with convective mediated heat transfer, may influence the system in a such way that the individual form factors f_i can be sensitive to the heat distribution along the gas, which in turn can imply in a dependence on the energy fluxes, or in other words,

$$f_i = g_i(p, W_1, W_2, \dots, W_N), \tag{8}$$

where $g_i(p, W_1, W_2, \dots, W_N)$ are $i = 1, \dots, N$ functions of the pressure p and of all the energy fluxes W_i ($i = 1, \dots, N$). In this case the linearity of Eq. 5 would be lost.

In order to express this mathematical formalism in a more suitable form for our experimental setup, we will start to consider a particular system in the subsection below.

Radiating heat exchange between two wires, in vacuum

This study is basically the experimental study of the exchange of heat between two wires, one of them being an electrically heated filament, and the other just being a thermocouple that receives heat radiation from the filament. They are sustained both parallel (at a distance d) and on the horizontal plane alongside the extension of a cylindrical tube (playing the role of a cavity). The electric filament irradiates heat at a rate W given by Joule’s law,

$$W = R \cdot I^2, \tag{9}$$

where R is the filament resistance and I is the electrical current. The fraction E of this heat that arrives to the thermocouple is determined by a simple geometric form factor, given by

$$E = \frac{c}{2\pi d} \cdot W = \frac{c}{2\pi d} \cdot RI^2, \tag{10}$$

where c is the thermocouple wire diameter. By the Stefan–Boltzmann law, $E = \sigma T_{tc}^4$, where T_{tc} is the thermocouple (irradiated wire) temperature. As a consequence,

$$\sigma T_{tc}^4 = \frac{c}{2\pi d} \cdot RI^2. \tag{11}$$

Now, we will consider the participation of a secondary source of heat irradiating at the time rate W_2 . Then,

$$\sigma T_{tc}^4 = \frac{c}{2\pi d} \cdot RI^2 + f_2 \cdot W_2, \tag{12}$$

where we have introduced a second form factor f_2 associated to the heat transfer from source W_2 to the thermocouple. In this study, we will see that this secondary source is just the external ambient thermal radiation, which represents a thermal flux of energy per unit area given by

$$W_2 = \sigma T_a^4, \tag{13}$$

where T_a is the ambient temperature (laboratory ambient temperature). Since, the thermocouple receives heat from all directions, it is easy to verify that $f_2 = 1$, so we arrive at

$$\sigma T_{tc}^4 = \frac{c}{2\pi d} \cdot RI^2 + \sigma T_a^4. \tag{14}$$

Of course the tube represents an additional source of heat, and we should add a third term to the second member

of Eq. 14. In particular, the tube inner walls are of course hotter than the external ambient, so its contribution to expression 14 is certainly more significant than σT_a^4 . However, we do not know what exactly is the tube temperature, especially when the tube is filled with a gas at a particular pressure, and convective phenomena give rise to a nonzero gradient of temperature along the inner walls of the tube. We can represent both the contributions from gas and tube radiances including an effective form factor $F(p, W)$ which in principle depends on the gas pressure p and on the filament radiance W , so we rewrite Eq. 14 as

$$\sigma T_{tc}^4 = F(p, W) \cdot \frac{c}{2\pi d} \cdot RI^2 + \sigma T_a^4 \tag{15}$$

or

$$T_{tc}^4 = \phi \cdot I^2 + T_a^4, \tag{16}$$

where we defined $\phi = \phi(p, I^2)$ as

$$\phi(p, I^2) = \frac{F(p, W)}{\sigma} \cdot \frac{c}{2\pi d} \cdot R. \tag{17}$$

By our above considerations, F and $\phi = \phi(p, I^2)$ are constant when there is no gas in the tube, and a plot of T_{tc}^4 as a function of I^2 will give a straight line. However, when there is gas in the tube, it is expected that they will depend on both the gas pressure p and on the filament energy flux W , so the dependence of T_{tc}^4 on I^2 will not yet be linear.

Experimental

The experimental measurements were made with a device specially made for this study, and it consisted of a cylindrical refractory glass tube (see Fig. 1a) 100 mm long and with internal diameter 20 mm. Inside the tube there was a thin filament 50 mm long along the tube axis. Parallel to it there was a thermocouple 5 mm away from the tube axis. The filament had 1.42×10^{-1} mm diameter and an electrical resistance $R_f = 4.2 \Omega$, which was verified that not varied with the electrical current in the range of currents used in this study. A steel spring kept the filament always straight despite its thermal dilatation. The thermocouple was 85 mm long and consisted of wires of iron (3.0×10^{-1} mm diameter) and constantan (5.0×10^{-1} mm diameter) with a conversion factor $a = 0.054 \text{ mV K}^{-1}$ in the range of temperatures of the experiment. The thermocouple junction was situated just in front of the middle of the filament.

One of the ends of the glass tube had an aperture connected to a vacuum system with control of the pressure of air inside of the tube, consisting of a vacuum pump, taps to control pressure and a liquid Hg column manometer for calibration and reference. To aid in the calibration of the manometer, we used a barometer with precision up to

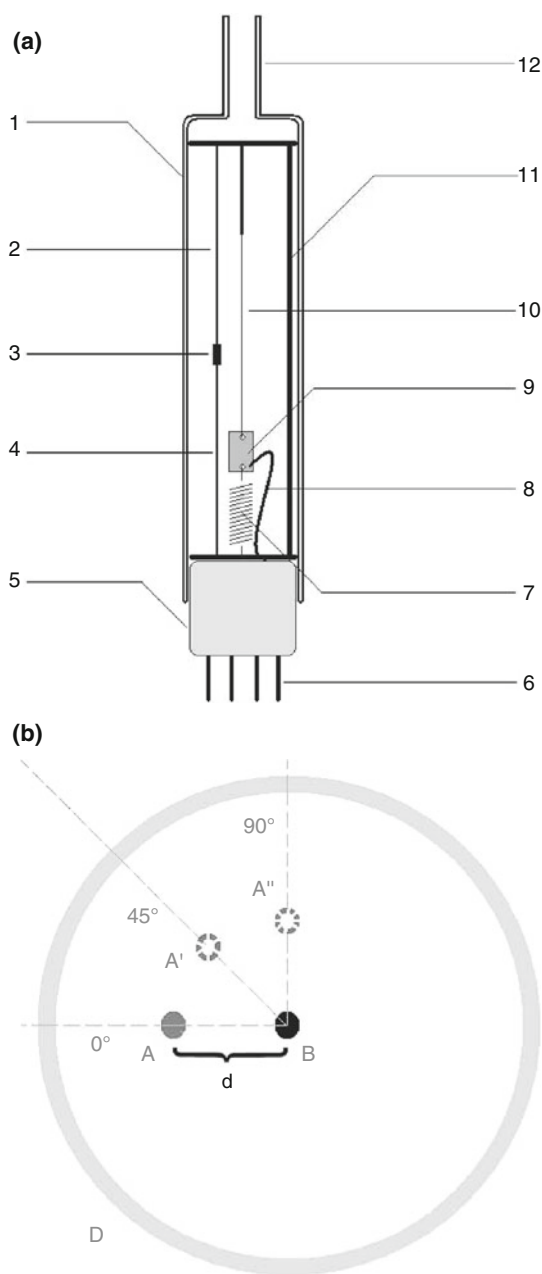


Fig. 1 *a* Schematic representation of the device: 1 glass tube; 2 thermocouple iron wire; 3 thermocouple junction; 4 thermocouple constantan wire; 5 tube sealing; 6 thermocouple and filament electrical connections; 7 steel spring; 8 electrical wiring for filament; 9 copper plate; 10 filament; 11 filament and thermocouple holder; 12 aperture to vacuum system. *b* Representation of the cross section of the glass tube (labeled by *D*) at the horizontal position, where the relative positions of the thermocouple (represented by *full*, *dashed* and *dotted gray* circles at positions labeled by *A*, *A'* and *A''*) is shown with respect to the filament (*black circle* labeled by *B*) at the three different angular orientations (0° , 45° , and 90° , respectively). *d* is the distance between the filament and the thermocouple

0.1 mbar provided atmospheric pressure. The other end of the tube was sealed and from this side the electrical connections of the filament and the thermocouple came out.

The electrical heating source of the filament was a 0–25.0 V d.c. controlled and stabilized source, where the voltage and current were measured by a voltmeter (precision up to 0.1 V), and a milliampèremeter (precision up to 1 mA). The thermocouple was connected to a millivoltmeter, with 0.1 mV precision and the ambient temperature T_a was read in a liquid Hg bulb thermometer at the laboratory, and it was verified that along all the experiment $T_a = (26 \pm 1)^\circ\text{C}$.

The thermocouple temperature was determined by the conversion formula $V_{tc} = a(T_{tc} - T_a)$, where V_{tc} is the electrical potential difference generated in the thermocouple, T_{tc} is the thermocouple temperature, and T_a is the ambient (laboratory) temperature.

Results

First, the measurements were made with the tube set on the horizontal position with both the filament and the thermocouple at the same horizontal plane. In a second stage of the experiment, the measurements were made with the tube turned around its axis, by the angle of 45° . In a third stage, the tube was turned again to complete a 90° rotation, in order that the thermocouple stood just above the filament. These three different stages of the experiment are represented in Fig. 1b and allowed studying the thermocouple temperature as a function of the convective heating of the air (when present) in the tube at different configurations.

Data collecting consisted of reading the thermocouple potential difference after step by step increase of filament voltage from 1.00 up to 7.00 V, for the minimum air pressure of 20–26 mbar. After a complete scan, the same was repeated with step by step increase of pressure up to 1000 mbar. In all the experiments, the maximum filament current was around 1.3 \AA to avoid damage by overheating.

The result was a set of successive curves relating the potential difference of the thermocouple V_{tc} and pressure p to each fixed filament voltage. For the first stage of the experiment where filament and thermocouple remained in the same horizontal plane, the corresponding experimental data are presented in Fig. 2. In this figure, it can be seen that the thermocouple potential difference shows a slow variation around all the studied range of pressures. Typically, the increase of pressure by almost three orders of magnitude (from 13 to 1035 mbar) represented only a decrease of 40% on the value of V_{tc} .

In order to check the behavior of experimental data with respect to the theory presented on the previous section, particularly referring to Eqs. 16 and 17, we have made a set of plots of T_{tc}^4 as a function of I^2 for fixed values of air pressure. For brevity, here we present only some of these plots.

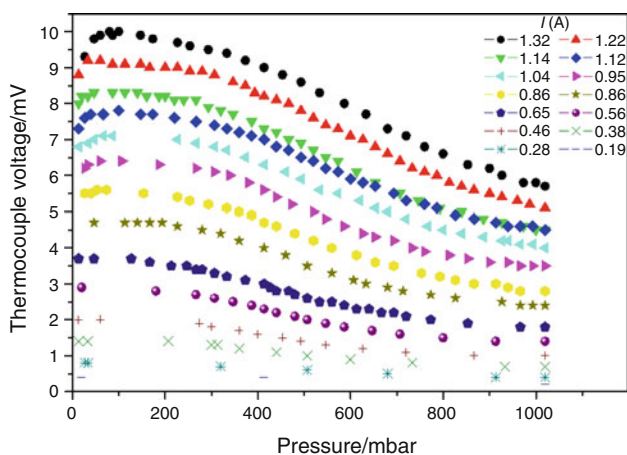


Fig. 2 (Color online) Plot of the experimental values of the thermocouple voltage (V_{tc}) as a function of the pressure in the tube (p). The *full circles* are the experimental data, and the linking lines are guide to the eyes. Each curve was obtained for a given fixed filament voltage, for which the corresponding filament currents are shown

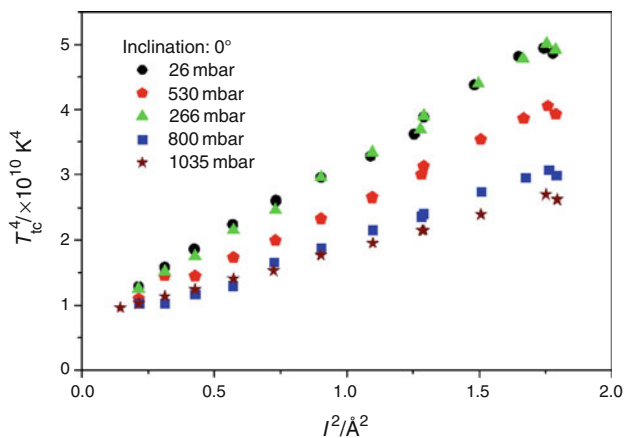


Fig. 3 (Color online) Plot of the fourth power of the thermocouple temperature (T_{tc}^4) as a function of the square of the filament current (I^2) with experimental data obtained on the first stage of the experiment (angle of rotation 0°) for five different gas pressures, where we can see clearly a linear behavior

In Fig. 3, we present the T_{tc}^4 versus I^2 plot corresponding to five different pressures in the range from 26 to 1035 mbar. We can clearly see the linear behavior in all sets of points. This reveals that in the theoretical formalism above presented the form factor ϕ varies only with the pressure.

Now, we pass to the second and third stages of the experiment, where the tube was rotated around its axis (as shown also in Fig. 1b). In Fig. 4, we present the T_{tc}^4 versus I^2 plots at different pressures and angles of rotation of the tube. In all these situations the dependence is linear, showing that the form factor ϕ does not depend on the filament current, and as a consequence, on the source (filament) energy flux W .

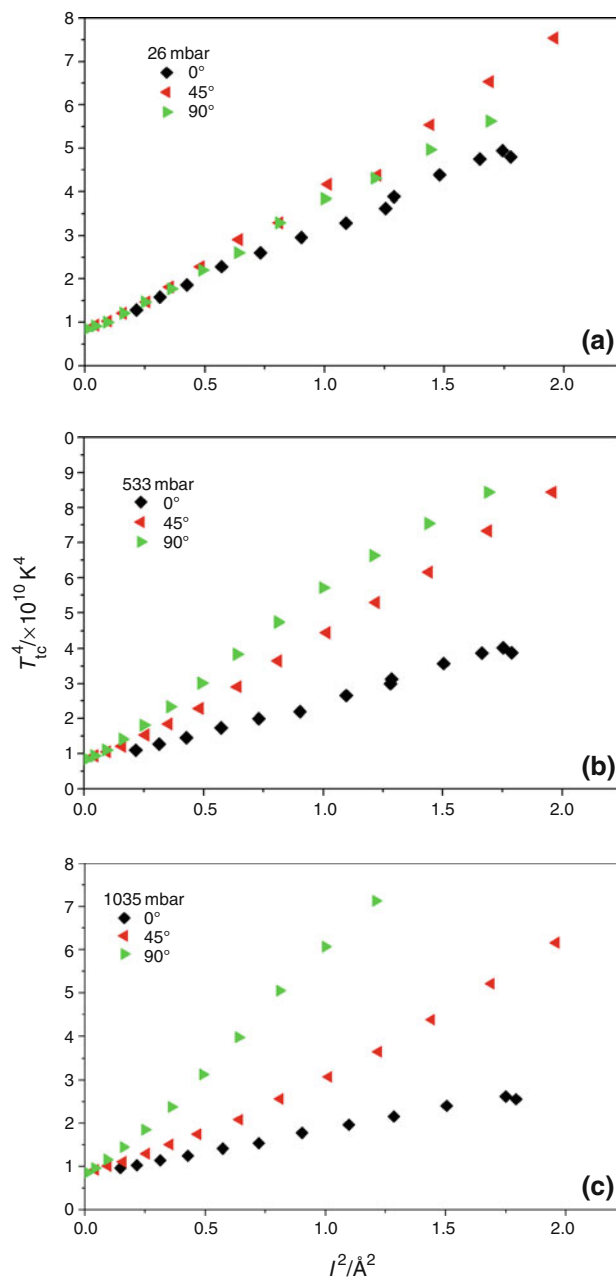


Fig. 4 (Color online) Plots of the fourth power of the thermocouple temperature (T_{tc}^4) as a function of the square of the filament current (I^2) for the different stages of the experiment, say, the angles of rotation of 0° , 45° , and 90° . **a** pressure: 26 mbar; **b** pressure: 533 mbar; and **c** pressure: 1035 mbar. As in Fig. 3, the experimental data follow a linear dependence

A point to stress here is the fact that as we decrease the filament current all the T_{tc}^4 versus I^2 curves converge to the same point, which coincide with the ambient (laboratory) temperature. In fact, this is not surprising, since at $I = 0$ evidently the thermocouple temperature must be equal to the ambient temperature, i.e., $T_{tc} = T_a$. In fact, the linear regression for all the curves gave $T_a = (24 \pm 3)^\circ\text{C}$, which

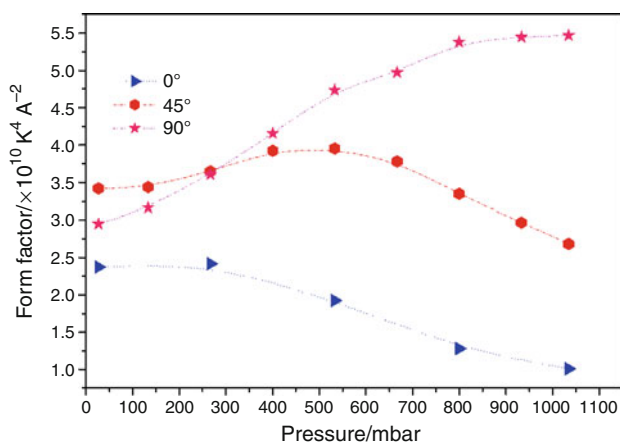


Fig. 5 (Color online) Plots of the form factor (ϕ) as a function of the gas pressure (p) for the different stages of the experiment, say, the angles of rotation of 0° (for which the dependence is monotonically decreasing), 45° (for which the dependence is a non monotonic transition mode), and 90° (for which the dependence is monotonically crescent)

is in good agreement with the value $T_a = (26 \pm 1)^\circ\text{C}$ previously mentioned.

At this moment it would be interesting to analyze the behavior of the form factor ϕ as the pressure was varied. In Fig. 5, we show the variation of ϕ as the pressure was increased, for the three different rotations of the tube. It can be seen that the angle of rotation strongly influences the value of ϕ . While for angle 0° the behavior is monotonically decreasing, the increase to 45° makes ϕ to have non-monotonic behavior, changing from crescent below 500 mbar to decrescent above 500 mbar. Finally, at 90° the behavior is strictly crescent.

Note that in our fittings we did not consider the thermal radiance contribution from the walls of the tube. This would represent the addition of a second energy flux source term W_2 , determined by the ratio of the total filament energy power RI^2 by the inner tube surface. At vacuum, the temperature of the wall of the tube T_w is determined simply by $\sigma T_w^4 = W_2$, but the presence of air creates a gradient of temperature along the wall of the tube due to convective phenomenon. This fact is not in contradiction with our results. On the contrary, even corroborates the finding that in the complex heat exchange mediated by the air the independence of ϕ with respect to the heat sources is preserved.

Conclusions

We verified that the form factor strongly depends on the air pressure but not on the source power itself. It was shown that the air inside the tube contributed in the heat exchanges in such a way that the thermal radiation received by the thermocouple was always determined by a constant fraction of the total thermal radiation emitted by the filament, for a given fixed air pressure. In other words, the system behaved as it had an “effective form factor”, independent of the source power.

In particular, the experiment was neither performed with dehumidified air nor pure or inert gases, so we can believe that the same result would be obtained with any gaseous mixture. An interesting study would be to repeat the experiment filling the tube with liquid material, for which we expect to arrive to the same results.

Acknowledgements The author thanks to prof. A.T.F. Amado for incentive and license for use of laboratory.

References

1. Roth A. Vacuum Technology. 3rd ed. Amsterdam: North-Holland Publishing Company; 1982.
2. Ellet A, Zabel RM. The Pirani Gauge for the measurement of small changes of pressure. *Phys Rev.* 1931;37:1102–11.
3. Sellenger FR. A review of vacuum gauges and methods for high vacuum gauge calibration. *Vacuum.* 1968;18:645–50.
4. Voegel W. *Phys Zeit.* 1906;7:498.
5. Steckelmacher W. The high pressure sensitivity extension of thermal conductivity gauges. *Vacuum.* 1973;23:307–11.
6. Duarte CA. A thermocouple vacuum gauge for low vacuum measurement. *Vacuum.* 2011;85:972–4.
7. Landau LD, Lifshitz EM. Statistical physics. Course of theoretical physics, vol 5, 3rd ed. Oxford: Butterworth-Heinemann; 1980.
8. Pérez-Madrid A, Rubí JM, Lapas LC. Non-equilibrium Stefan-Boltzmann law. *J Non Equilib Thermodyn.* 2010;35:279–88.
9. Landau LD, Lifshitz EM. Fluid mechanics. Course of theoretical physics, vol 6, 2nd ed. Oxford: Butterworth-Heinemann; 1987.
10. Sieniutycz S. Identification and selection of unconstrained controls in power systems propelled by heat and mass transfer. *Int J Heat Mass Transf.* 2011;54:938–48.
11. Cheng X, Liang X. Entransy flux of thermal radiation and its application to enclosures with opaque surfaces. *Int J Heat Mass Transf.* 2011;54:269–78.